

Physical mechanism of oxygen diffusion in the formation of Ga_2O_3 Ohmic contacts

Su-Yu Xu(徐宿雨), Miao Yu(于淼), Dong-Yang Yuan(袁东阳), Bo Peng(彭博), Lei Yuan(元磊), Yu-Ming Zhang(张玉明), and Ren-Xu Jia(贾仁需)

Citation: Chin. Phys. B, 2024, 33 (**1**): 017302. DOI: 10.1088/1674-1056/ad01a7
Journal homepage: http://cpb.iphy.ac.cn; http://iopscience.iop.org/cpb

What follows is a list of articles you may be interested in

A self-powered ultraviolet photodetector based on a Ga_2O_3/Bi_2WO_6 heterojunction with low noise and stable photoresponse

Li-Li Yang(杨莉莉), Yu-Si Peng(彭宇思), Zeng Liu(刘增), Mao-Lin Zhang(张茂林),Yu-Feng Guo(郭宇锋), Yong Yang(杨勇), and Wei-Hua Tang(唐为华)

Chin. Phys. B, 2023, 32 (**4**): 047301. DOI: 10.1088/1674-1056/ac7865

Design and research of normally-off *β*-Ga_2O_3/4H-SiC heterojunction field effect transistor

Meixia Cheng(程梅霞), Suzhen Luan(栾苏珍), Hailin Wang(王海林), and Renxu Jia(贾仁需)

Chin. Phys. B, 2023, 32 (**3**): 037302. DOI: 10.1088/1674-1056/aca39c

Effects of preparation parameters on growth and properties of *β*-Ga_2O_3 film

Zi-Hao Chen(陈子豪), Yong-Sheng Wang(王永胜), Ning Zhang(张宁), Bin Zhou(周兵), Jie Gao(高洁), Yan-Xia Wu(吴艳霞), Yong Ma(马永), Hong-Jun Hei(黑鸿君), Yan-Yan Shen(申艳艳), Zhi-Yong He(贺志勇), and Sheng-Wang Yu(于盛旺)

Chin. Phys. B, 2023, 32 (**1**): 017301. DOI: 10.1088/1674-1056/ac728c

Steady-state and transient electronic transport properties of *β*-$(Al_xGa_{1-x})_2O_3/Ga_2O_3$ heterostructures: An ensemble Monte Carlo simulation

Yan Liu(刘妍), Ping Wang(王平), Ting Yang(杨婷), Qian Wu(吴茜), Yintang Yang(杨银堂), and Zhiyong Zhang(张志勇)

Chin. Phys. B, 2022, 31 (**11**): 117305. DOI: 10.1088/1674-1056/ac7290

Lateral *β*-Ga_2O_3 Schottky barrier diode fabricated on (-201) single crystal substrate and its temperature-dependent current-voltage characteristics

Pei-Pei Ma(马培培), Jun Zheng(郑军), Ya-Bao Zhang(张亚宝), Xiang-Quan Liu(刘香全), Zhi Liu(刘智), Yu-Hua Zuo(左玉华), Chun-Lai Xue(薛春来), and Bu-Wen Cheng(成步文)

Chin. Phys. B, 2022, 31 (**4**): 047302. DOI: 10.1088/1674-1056/ac2729

Physical mechanism of oxygen diffusion in the formation of Ga_2O_3 Ohmic contacts

Su-Yu Xu(徐宿雨)[1], Miao Yu(于淼)[1,†], Dong-Yang Yuan(袁东阳)[2], Bo Peng(彭博)[1], Lei Yuan(元磊)[1], Yu-Ming Zhang(张玉明)[1], and Ren-Xu Jia(贾仁需)[1,‡]

[1] *Key Laboratory of Wide Band-Gap Semiconductor Materials and Devices, School of Microelectronics, Xidian University, Xi'an* 710071, *China*
[2] *The* 13*th Research Institute China Electronics Technology Group Corporation, Shijiazhuang* 050051, *China*

(Received 2 August 2023; revised manuscript received 18 September 2023; accepted manuscript online 7 October 2023)

The formation of low-resistance Ohmic contacts in Ga_2O_3 is crucial for high-performance electronic devices. Conventionally, a titanium/gold (Ti/Au) electrode is rapidly annealed to achieve Ohmic contacts, resulting in mutual diffusion of atoms at the interface. However, the specific role of diffusing elements in Ohmic contact formation remains unclear. In this work, we investigate the contribution of oxygen atom diffusion to the formation of Ohmic contacts in Ga_2O_3. We prepare a Ti/Au electrode on a single crystal substrate and conduct a series of electrical and structural characterizations. Using density functional theory, we construct a model of the interface and calculate the charge density, partial density of states, planar electrostatic potential energy, and *I*–*V* characteristics. Our results demonstrate that the oxygen atom diffusion effectively reduces the interface barrier, leading to low-resistance Ohmic contacts in Ga_2O_3. These findings provide valuable insights into the underlying mechanisms of Ohmic contact formation and highlight the importance of considering the oxygen atom diffusion in the design of Ga_2O_3-based electronic devices.

Keywords: Ga_2O_3, Ohmic contacts, oxygen diffusion, density functional theory

PACS: 73.61.Le, 73.40.Ns, 66.30.J–, 71.15.Mb **DOI:** 10.1088/1674-1056/ad01a7

1. Introduction

Gallium oxide (Ga_2O_3) is an ultra-wide bandgap semiconductor material that has garnered significant attention as a candidate for next-generation power electronics and optoelectronic devices.[1–10] It is characterized by its excellent chemical and thermal stability, high visible light transmission rate, and Si-compatible preparation process that enables mass production. Nevertheless, the development of Ga_2O_3-based devices is still in its infancy, and numerous challenges, including the formation of good Ohmic contacts, persist.[11–16] The formation of Ohmic contacts between metal electrodes and semiconductors is a fundamental prerequisite for any semiconductor device to operate successfully. The magnitude of the contact resistance between the metal and semiconductor is a crucial factor that influences the performance of the device, particularly its power, noise frequency, and thermal stability. However, the precise mechanism governing the formation of Ohmic contacts between metals and Ga_2O_3 remains incompletely understood. Prior research has demonstrated that the Au-covered Ti (Ti/Au) electrode, annealed at 400 °C, exhibits the lowest Ohmic contact resistance with Ga_2O_3, and thus is the most commonly used approach to achieve Ohmic contact with gallium oxide.[17–21] Although the rapid annealing of Ti/Au electrodes is known to result in interdiffusion at the interface between the electrode and Ga_2O_3, the exact role played by the diffusion of various elements in the formation of Ohmic contacts in Ga_2O_3 is not yet clear.[22] As oxygen diffusion is the most pronounced interfacial diffusion, studying the contribution of oxygen element diffusion to the formation of Ohmic contacts is critical for gallium oxide.

This study investigates the contribution of oxygen atom diffusion to the formation of Ohmic contacts in Ga_2O_3. Specifically, we prepared titanium/gold electrodes on a single crystal gallium oxide substrate and evaluated their current-voltage characteristics, energy dispersive x-ray elemental mapping spectrum, and electron energy loss spectroscopy. We constructed interface models of gallium oxide and titanium and calculated their charge density, partial density of state, planar electrostatic potential energy, and current–voltage characteristics. Our results reveal that oxygen atoms at the Ga_2O_3 interface diffuse into the titanium layer, where they oxidize the Ti and leave oxygen vacancies near the interface. The presence of these vacancies lowers the interfacial potential barrier, enhances the overlap degree of electron cloud at the interface, and ultimately facilitates the flow of electrons across the interfacial potential barrier, enabling Ohmic properties. These findings provide valuable insights into the underlying mechanisms governing the formation of Ohmic contacts and underscore the importance of considering oxygen atom diffusion in

†Corresponding author. E-mail: myuxidian@163.com
‡Corresponding author. E-mail: rxjia@mail.xidian.edu.cn

© 2024 Chinese Physical Society and IOP Publishing Ltd

the design of Ga_2O_3-based electronic devices.

2. Methods

The Ti/Au electrodes were deposited on a single crystal commercial Ga_2O_3 substrate with a $(\bar{2}01)$ phase using direct current magnetron sputtering. The Ti electrode was sputtered at a power of 50 W for 1200 s, while the Au electrode was sputtered at a power of 20 W for 3600 s. In this work, the thickness of Ti is about 50 nm and the thickness of Au is about 110 nm. Subsequently, the samples underwent rapid thermal annealing (RTA) for 120 s under a nitrogen atmosphere at an annealing temperature of 470 °C, in accordance with established protocols.[22] The current–voltage (I–V) characteristics were measured using a cascade probe table fitted with an Agilent B1500A. The structural and elemental features of the electrodes and the interface were characterized using Thermo Scientific Tecnai F20 transmission electron microscopy. In this study, all calculations were performed using density functional theory with the linear combination of atomic orbitals (LCAO) method, as implemented in the Quantum ATK package. The MGGA-TB09 exchange–correlation functional was employed to describe the exchange–correlation energy between electrons, while the PseudoDojo pseudopotential was used to model the electron–ion interaction potential.[23,24] Brillouin zone integration in reciprocal space was carried out using a grid density of k-points of $12 \times 2 \times 1$, and the cut-off energy was set to 550 eV. The convergence criteria for energy, force, stress, and displacement during the calculations were set at 5×10^{-6} eV, 0.03 eV/Å, 0.02 GPa, and 5×10^{-4} Å, respectively, to ensure high accuracy and reliability of the results.

3. Results and discussion

In this study, we fabricated Ti/Au electrodes on a single crystal Ga_2O_3 substrate oriented along the $(\bar{2}01)$ direction. The electrical behavior of the device before and after rapid thermal annealing (RTA) was evaluated using I–V measurements, as illustrated in Fig. 1(a). The I–V curve prior to RTA exhibited distinct Schottky characteristics, while the I–V curve following RTA displayed clear Ohmic behavior, indicating a significant change in the quality of the interface. To determine the specific contact resistance of the RTA-treated sample, we employed the transmission line model (TLM) method.[25] The electrode structure utilized for this measurement is depicted in Fig. 1(b). By varying the electrode spacing, we obtained the I–V characteristics as shown in Fig. 1(c), from which we extracted the specific contact resistance ρ_c and plotted it against electrode spacing, as shown in Fig. 1(d). The specific contact resistance of the RTA-treated sample was found to be 2.21×10^{-5} Ω·cm^2. These results reveal that the initial Ti/Ga_2O_3 contact is Schottky in nature, and that the RTA treatment is critical in transforming it to an Ohmic contact. The change in the electrical behavior of the interface is likely attributed to the reduction of the barrier height at the Ti/Ga_2O_3 junction caused by the thermal treatment.

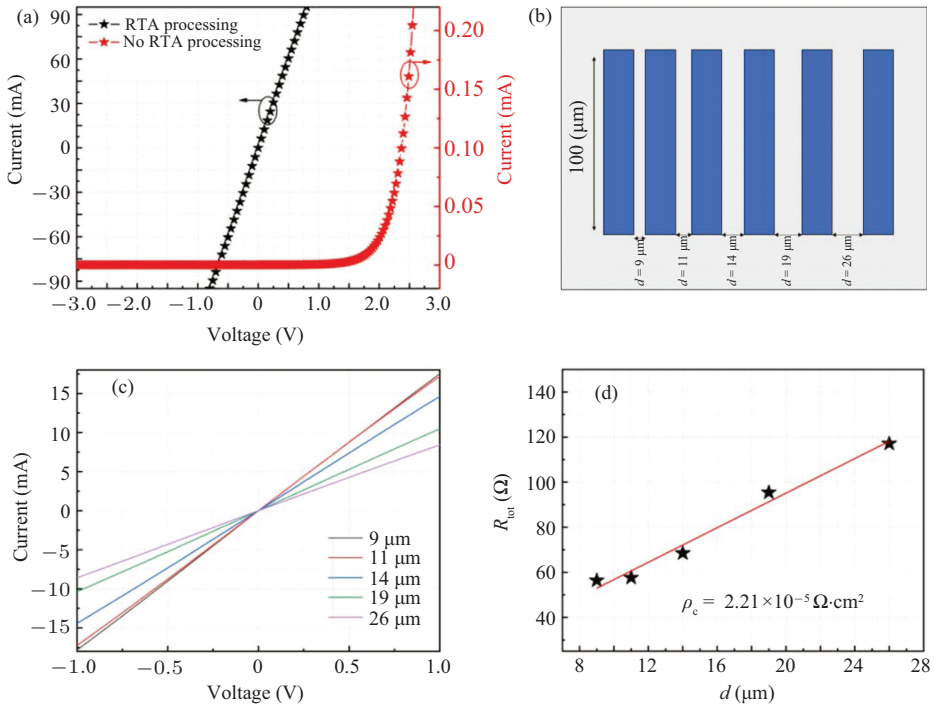


Fig. 1. (a) Comparison of I–V characteristics for Ti/Au electrodes with and without rapid annealing; (b) electrode structure for contact resistance measurement using TLM method; (c) effect of electrode spacing on I–V characteristics; (d) fitting curve for extracting contact resistance of Ti/Au electrodes.

Figure 2 displays the x-ray photoelectron spectroscopy (XPS) spectrum of the interface between Ti and Ga_2O_3 in the unannealed sample. The binding energies of all peaks are calibrated to the C 1s peak located at 284.8 eV. The spectrum exhibits distinct peaks of Ga at approximately 1116 eV, O at approximately 530 eV, and Ti at approximately 460 eV. The XPS spectrum of Ti at the interface is presented in the inset, revealing a double-peak spacing of 5.7 eV between the Ti $2p_{1/2}$ and Ti $2p_{3/2}$ orbital peaks. This indicates that Ti in its elemental state is present at the interface of the unannealed sample, and no reactions have occurred at the interface.[26]

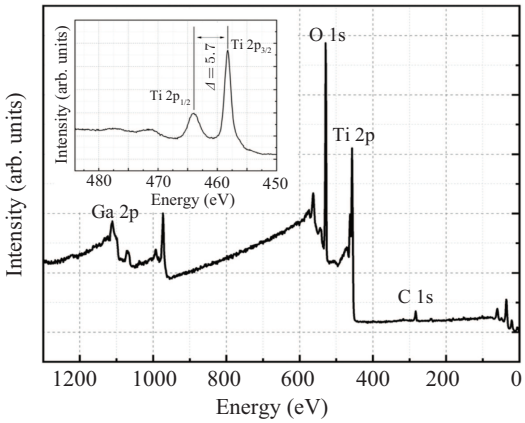


Fig. 2. The XPS analysis of the interface between unannealed Ti and Ga_2O_3, with insert showing the Ti XPS spectrum at the interface.

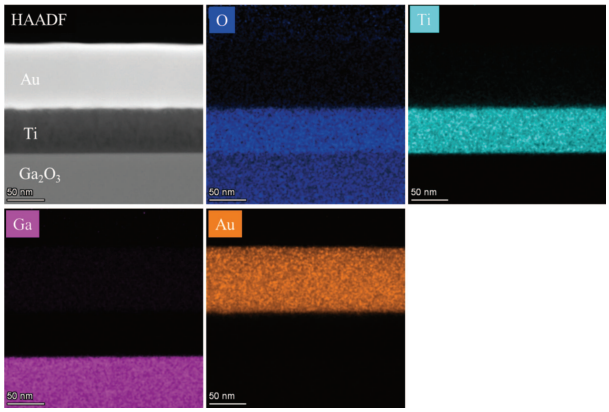


Fig. 3. The EDX elemental mapping spectrum of the Ti/Au–Ga_2O_3 interface after rapid thermal annealing.

The energy-dispersive x-ray (EDX) element mapping spectrum of the annealed sample is displayed in Fig. 3. The spectrum demonstrates the distribution of O, Ti, Ga, and Au elements. The deep blue area indicates the distribution of O elements, the light blue area indicates the distribution of Ti elements, the purple area indicates the distribution of Ga elements, and the orange area indicates the distribution of Au elements. It is evident that a substantial amount of oxygen exists in the Ti metal layer at the interface. To further examine the valence state of Ti at the interface, we conducted electron energy loss spectroscopy (EELS) on the sample after rapid thermal annealing and thoroughly analyzed the high-energy loss region of the EELS.[27,28]

The EELS results are illustrated in Fig. 4, where the three peak values marked as A, B, and C correspond to energy values of 458.3 eV, 460.7 eV, and 463.3 eV, respectively. These results demonstrate that the Ti at the interface is in the Ti^{3+} state after rapid annealing.[29]

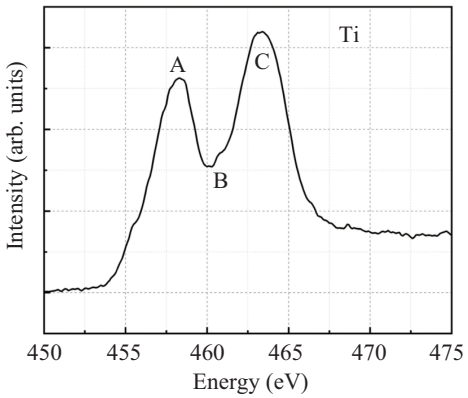


Fig. 4. The electron energy loss spectroscopy of Ti at the Ti/Au interface after rapid annealing.

Table 1 presents the elemental proportion distribution of the Ga_2O_3 layer at the interface. The O-to-Ga ratio is close to 1:1, much less than 2:3. Since the preparation and structural characterization of the sample were carried out under anoxic conditions, the oxygen in the Ti layer is attributed to the diffusion of oxygen atoms in the Ga_2O_3 caused by rapid annealing. The findings of the related tests support this hypothesis. The current–voltage testing results, when combined with the previously discussed results, indicate that rapid annealing changes the Ti/Au electrode and Ga_2O_3 from a Schottky contact to an Ohmic contact. The diffusion of oxygen atoms at the interface can be regarded as the most prominent change caused by rapid annealing. This indicates that the diffusion of oxygen at the interface of Ga_2O_3 may have a significant influence on the formation of Ohmic contact.

Table 1. Element ratio distribution at the Ti/Au–Ga_2O_3 interface after rapid annealing.

Element	Atomic fraction (%)	Atomic error (%)	Mass fraction (%)	Mass error (%)
O	48.9	8.19	18.56	1.97
Ti	0.16	0.03	0.17	0.03
Ga	49.86	10.49	80.83	13.68
Au	0.1	0.02	0.44	0.07

To investigate the impact of interfacial oxygen diffusion on the formation of Ohmic contact between Ti and gallium oxide, we selected the $(\bar{2}01)$ crystal phase of gallium oxide and the (100) crystal phase of Ti to construct various nanodevice models with different contact interfaces. Prior to building the interface models, we optimized the Ga_2O_3 bulk material, and the results are illustrated in Fig. 5(a). The bulk material parameters, namely $a = 12.43$ Å, $b = 3.08$ Å, $c = 5.87$ Å, $\alpha = \gamma = 90°$, and $\beta = 103.68°$, respectively, were determined. Furthermore, the energy band structure of Ga_2O_3 is depicted in Fig. 5(b), revealing a quasi-direct band gap of 4.87 eV. Both the lattice constant and the band gap width are consistent with previously reported experimental and calculated values.[30–32]

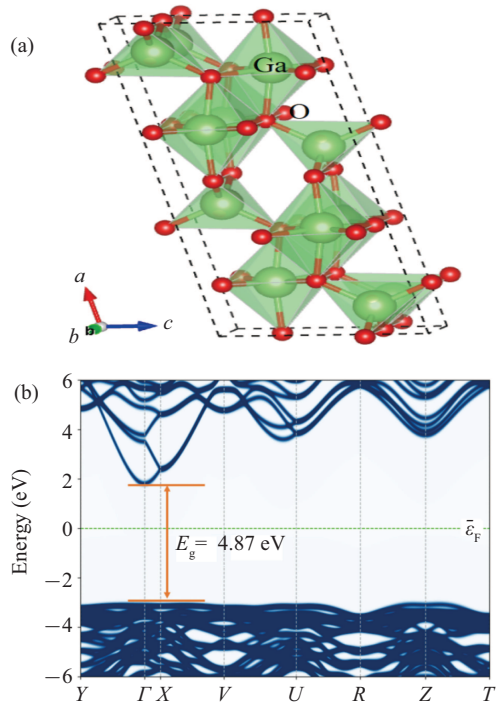


Fig. 5. Lattice structure (a) and band structure (b) of gallium oxide bulk material.

After optimizing the lattice structure of Ga_2O_3, we used 5 layers of Ga_2O_3 in the $(\bar{2}01)$ direction and 5 layers of Ti in the (100) direction as metal electrodes to build a device model. The parameter of the device model is $a = 3.08$ Å, $b = 14.96$ Å, $c = 37$ Å, $\alpha = \beta = \gamma = 90°$. Our study involved the generation of three interface models to describe the interaction between Ga_2O_3 and Ti. These models included a direct contact model, a low concentration oxygen diffusion model, and a high concentration oxygen diffusion model. The direct contact model (M-direct) describes the absence of oxygen atom diffusion into the Ti layer upon contact with Ga_2O_3. In contrast, the low concentration oxygen diffusion model (M-low) represents the diffusion of oxygen atoms at a low concentration into the Ti layer, while the high concentration oxygen diffusion model (M-high) represents the diffusion of oxygen atoms at a high concentration into the Ti layer. The interface model between Ti and Ga_2O_3 in direct contact is depicted in Fig. 6(a). Due to differences in lattice constants, the interface experiences a slight degree of lattice distortion, while remaining well-matched. Figures 6(b) and 6(c) illustrate the oxygen diffusion models. Oxygen atoms from Ga_2O_3 diffuse into the Ti layer, leaving oxygen vacancies at the interface. Figure 6(b) represents oxygen diffusion at a low concentration, with one oxygen atom diffusing into the Ti layer. Figure 6(c) represents oxygen diffusion at a high concentration, with two oxygen atoms diffusing into the Ti layer. In M-low, the Ti atoms at the oxygen vacancies move towards adjacent Ti atoms and share an oxygen atom with them, thus pulling the oxygen atoms on the Ga_2O_3 side towards the Ti layer. In contrast, M-high is characterized by a more significant lattice distortion at the interface due to the Ti atoms moving larger distances. Ti atoms at the vacant sites take oxygen atoms from the deeper layers of Ga_2O_3, leading to a more pronounced tendency towards mutual diffusion at the interface. The high reactivity of Ti with oxygen results in Ti being more reductive than Ga.[33] Rapid annealing tends to move oxygen atoms towards the Ti layer, leading to the diffusion of oxygen atoms at the interface.

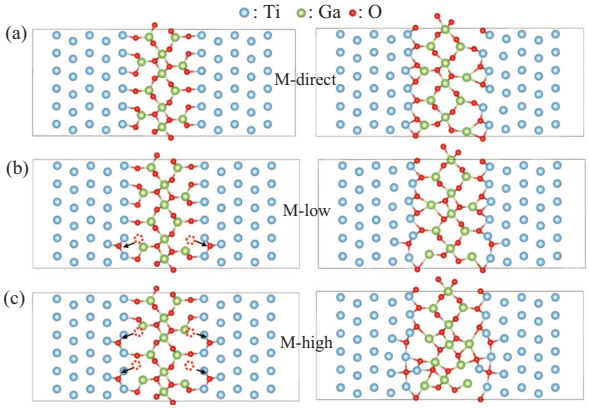


Fig. 6. Optimization of Ga_2O_3/Ti interface model with varying oxygen diffusion concentrations. (M-direct: no oxygen diffusion, M-low: low oxygen diffusion concentration, M-high: high oxygen diffusion concentration).

Electron cloud density is a key electronic property that characterizes the spatial distribution of electrons in a material. It quantifies the probability of finding an electron at a given point in space and is a fundamental parameter for understanding the electronic structure of materials.[34] Figure 7 presents the electron cloud density distributions for three distinct systems, namely, M-direct, M-low, and M-high, which are shown in panels (a), (b), and (c), respectively. The yellow regions in the figure represent the areas with non-zero electron cloud density, while the equivalence surface of the electron cloud density is set to a constant value of 0.025 e/Bohr^3 for all systems, thereby enabling a direct comparison of the electron cloud distributions across the different systems. Fluctuations in the electron cloud density at the interface have a significant impact on the barrier height. Our results reveal that M-low and M-high exhibit significantly higher electron density at the interface as compared to M-direct, indicating that there are more

available electron orbitals near the interface that facilitate easier electron transport between the two materials. Specifically, the presence of oxygen atoms on the surface of Ga_2O_3 entering the Ti layer contributes to an increase in the electron cloud density at the interface, resulting in the formation of new electron orbitals that enable electron transport between the interfaces.

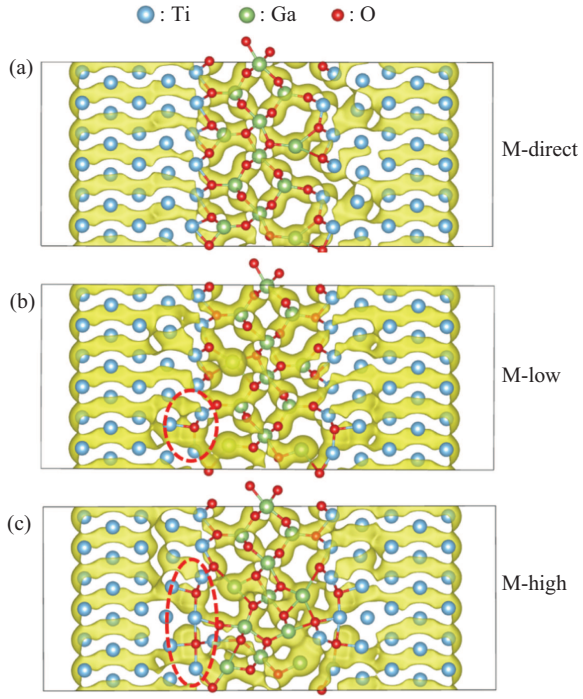


Fig. 7. Distribution of electron cloud density for Ga_2O_3/Ti interface models with varying oxygen diffusion concentrations. (a) M-direct: no oxygen diffusion, (b) M-low: low oxygen diffusion concentration, and (c) M-high: high oxygen diffusion concentration.

In order to conduct a thorough analysis of the impact of diffusing oxygen atoms at the interface on the electronic structure of the system during electron transport, we have performed calculations of the partial density of states (PDOS) at the interface. The PDOS results for M-direct, M-low, and M-high are presented in Figs. 8(a), 8(b), and 8(c), respectively. Given that the conduction band electrons at the interface mainly stem from Ti-3d orbital electrons and the valence band electrons are primarily contributed by O-2p orbital electrons, we have focused our investigation on these two regions. The density of states for O-2p and Ti-3d electrons in the M-direct, M-low, and M-high systems are depicted in Fig. 8(d). For the M-direct system, the cut-off energy of O-2p orbital electrons is −5.30 eV, and that of Ti-3d orbital electrons is −3.23 eV, giving rise to a potential barrier of 2.07 eV. Analogously, the potential barrier between O-2p orbital electrons and Ti-3d orbital electrons for the M-low system is 1.80 eV, and that for the M-high system is 0.58 eV. The results demonstrate that the diffusion of oxygen atoms into the Ti layer at the interface leads to a reduction in the potential barrier for electron transport, and this reduction becomes more pronounced as the concentration of diffusing oxygen atoms increases. This phenomenon arises due to the creation of new electron-occupied states for O-2p orbital electrons in Ga_2O_3 at higher energy levels, resulting from the oxygen vacancies that are formed by the oxygen atoms at the interface. Concurrently, the oxygen atoms that enter the Ti layer combine with Ti to generate new electron-occupied states for Ti-3d orbital electrons at lower energy levels, thereby decreasing the potential barrier, which promotes the formation of Ohmic properties. The diffusion of oxygen atoms at the interface is a promising strategy for effectively reducing the interfacial potential barrier of the Ti–Ga_2O_3 interface.

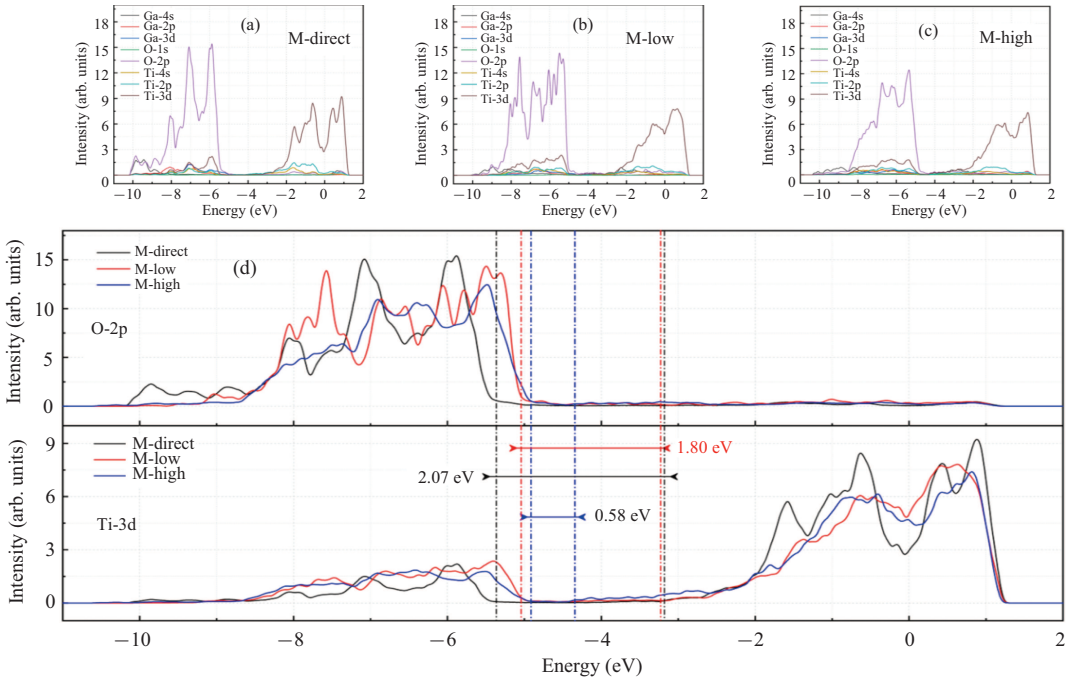


Fig. 8. Partial density of states (PDOS) at the Ga_2O_3/Ti interface with varying oxygen diffusion concentrations. (a) PDOS for M-direct, (b) PDOS for M-low, (c) PDOS for M-high, and (d) PDOS of O-2p orbital electrons and Ti-3d orbital electrons at the interface for M-direct, M-low, and M-high.

The planar electrostatic potential was calculated for different interface models, and the results are presented in Fig. 9(a). The differences in electrostatic potential between Ti and Ga_2O_3 in M-direct, M-low, and M-high are 5.35 eV, 4.9 eV, and 4 eV respectively. Upon contact, a notable potential difference was observed between the Ti and Ga_2O_3 interfaces, with the Ga_2O_3 side exhibiting a lower potential. This phenomenon indicates that free electrons from the Ga_2O_3 migrated towards the Ti, generating a built-in electric field that demonstrated Schottky properties. Comparatively, the potential difference between M-low and M-high interfaces was significantly lower than that of M-direct. Furthermore, the greater the concentration of diffused oxygen atoms, the more pronounced the potential difference reduction, which was consistent with density of states calculations. The planar electrostatic potential is directly linked to the charge transferred at the interface. To determine this, Bader charges of M-direct, M-low, and M-high at the interface were calculated, and the results are presented in Fig. 9(b). The Bader charge values of M-low, and M-high are 10.62 *e*, 8.75 *e*, and 7.80 *e* respectively. The charge transferred at the interface was significantly lower for M-low and M-high compared to M-direct. This was due to the bonding of oxygen atoms with Ti atoms in the Ti layer, which resulted in a reduction in the number of charges transferred at the interface, thereby lowering the potential difference at the interface.

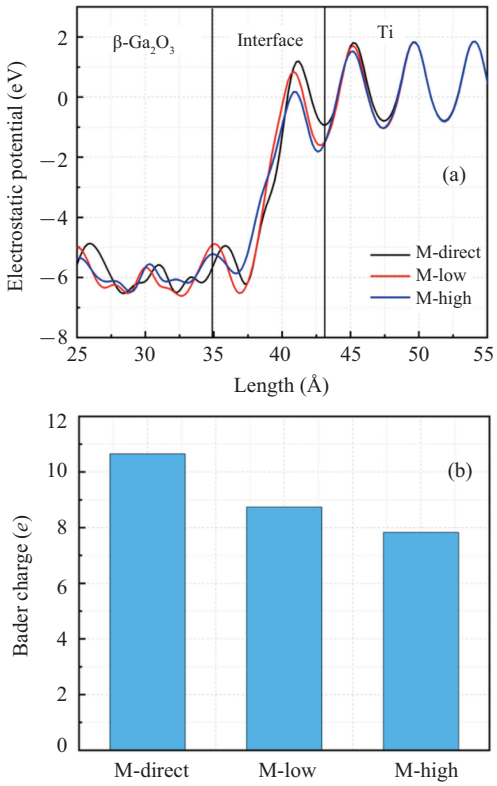


Fig. 9. Planar electrostatic potential and Bader charge at the interface between Ga_2O_3 and Ti for M-direct, M-low, and M-high models.

We employed a combined approach based on density functional theory and non-equilibrium Green's function to investigate the current–voltage (*I*–*V*) characteristics of M-direct, M-low, and M-high systems.[35,36] The results, presented in Fig. 10, indicate a distinct difference in the *I*–*V* behavior between the three systems. Specifically, the *I*–*V* curve of M-direct exhibited a Schottky-like behavior with an order of magnitude smaller current compared to that of M-low and M-high. This observation strongly suggests the presence of a Schottky contact at the interface between Ti and Ga_2O_3 in direct contact. In contrast, M-low and M-high displayed distinct Ohmic characteristics, with the *I*–*V* curve's slope for M-low being lower than that of M-high, indicating a lower contact resistance and superior Ohmic properties. Our theoretical analysis further revealed that the observed interfacial characteristics can be attributed to the diffusion of oxygen atoms from the Ga_2O_3 surface into the Ti layer. This process creates new electron orbitals at the interface, lowering the interfacial barrier, and increasing the probability of electron tunneling at the interface, resulting in the Ohmic behavior observed in M-low and M-high. Our findings highlight the importance of oxygen diffusion in tuning the interfacial properties of the Ti/Ga_2O_3 system and provide new insights into the design of high-performance electronic devices.

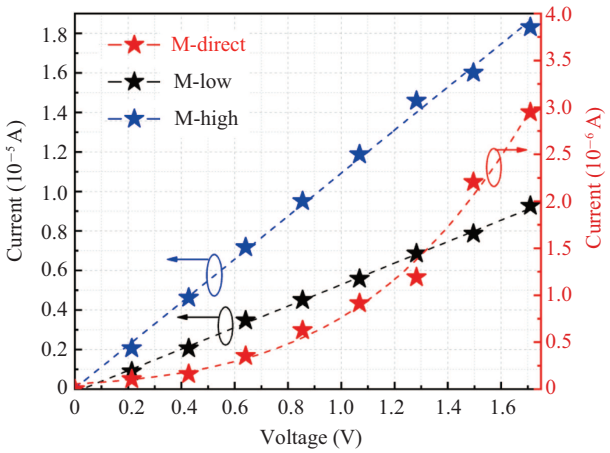


Fig. 10. First principles calculation of the current–voltage characteristics for Ga_2O_3/Ti interface models with varying oxygen diffusion concentrations.

4. Conclusion

In this investigation, we examined the critical role of oxygen diffusion in the development of Ohmic contact between Ti and Ga_2O_3. Specifically, we fabricated Ti/Au electrodes on single crystal Ga_2O_3 substrates, and our results revealed that direct contact between Ti and Ga_2O_3 is initially Schottky in nature, transitioning to Ohmic behavior after rapid thermal annealing (RTA). We further observed via energy-dispersive x-ray spectroscopy (EDX) and electron energy loss spectroscopy (EELS) the diffusion of oxygen atoms from Ga_2O_3 into the titanium layer after RTA, which caused the Ti to oxidize to a +3-valence state. To gain deeper insights into the underlying mechanisms driving the formation of Ohmic contacts, we

employed density functional theory to construct several interface models. Our analysis of charge density, partial density of state, planar electrostatic potential energy, and *I–V* characteristic calculations showed that oxygen diffusion decreases the interface potential barrier and enhances electron tunneling through the interface potential barrier. These outcomes explain the observed Ohmic behavior of the Ti/Ga_2O_3 system. The experimental findings were in good agreement with the calculated results. This study provides valuable insights into the mechanisms behind the formation of Ohmic contacts between Ti and Ga_2O_3, which could have implications for the development of high-performance electronic devices. Further studies could explore the impact of variations in processing parameters on the formation and properties of Ohmic contacts.

Acknowledgment

Projects supported by the National Natural Science Foundation of China (Grant Nos. 61874084, 61974119, and U21A20501).

References

[1] Guo D, Guo Q, Chen Z, Wu Z, Li P and Tang W 2019 *Mater. Today Phys.* **11** 100157
[2] Pearton S J, Yang J, Cary P H, Ren F, Kim J, Tadjer M J and Mastro M A 2018 *Appl. Phys. Rev.* **5** 011301
[3] Higashiwaki M and Jessen G H 2018 *Appl. Phys. Lett.* **112** 060401
[4] Galazka Z 2018 *Semicond. Sci. Technol.* **33** 113001
[5] Higashiwaki M, Murakami H, Kumagai Y and Kuramata A 2016 *J. Appl. Phys.* **55** 1202
[6] Ueda N, Hosono H, Waseda R and Kawazoe H 1997 *Appl. Phys. Lett.* **70** 3561
[7] Víllora E G, Shimamura K, Yoshikawa Y, Ujiie T and Aoki K 2008 *Appl. Phys. Lett.* **92** 202120
[8] Suzuki N, Ohira S, Tanaka M, Sugawara T, Nakajima K and Shishido T 2007 *Phys. Status Solidi C* **4** 2310
[9] Ohira S, Suzuki N, Arai N, Tanaka M, Sugawara T, Nakajima K and Shishido T 2008 *Thin Solid Films* **516** 5763
[10] Ahmadi E, Koksaldi O S, Kaun S W, Oshima Y, Short D B, Mishra U K and Speck J S 2017 *Appl. Phys. Express* **10** 041102
[11] Hwang W S, Verma A, Peelaers H, Protasenko V, Rouvimov S, Seabaugh A, Haensch W, de Walle C V, Galazka Z, Albrecht M, Fornari R and Jena D 2014 *Appl. Phys. Lett.* **104** 203111
[12] Higashiwaki M, Sasaki K, Kamimura T, Wong M H and Krishnamurthy D 2013 *Appl. Phys. Lett.* **103** 123511
[13] Chang P C, Fan Z, Tseng W Y, Rajagopal A and Lu J G 2005 *Appl. Phys. Lett.* **87** 222102
[14] Farzana E, Zhang Z, Paul P K, Arehart A R and Ringel S A 2017 *Appl. Phys. Lett.* **110** 202102
[15] Mann D, Javey A, Kong J, Wang Q and Dai H 2003 *Nano Lett.* **3** 1541
[16] English C D, Shine G, Dorgan V E, Saraswat K C and Pop E 2016 *Nano Lett.* **16** 3824
[17] Yao Y, Davis R F and Porter L M 2017 *J. Electron. Mater.* **46** 2053
[18] Chen J X, Li X X, Ma H P, Huang W, Ji Z G, Xia C, Lu H L and Zhang D W 2019 *ACS Appl. Mater. Interfaces* **11** 32127
[19] Xia Z, Joishi C, Krishnamoorthy S, Bajaj S, Zhang Y, Brenner M, Lodha S and Rajan S 2018 *IEEE Electron Dev. Lett.* **39** 568
[20] Carey P H, Yang J, Ren F, Hays D C, Pearton S J, Jang S, Kuramata A and Kravchenko I I 2017 *AIP Adv.* **7** 095313
[21] Sasaki K, Higashiwaki M, Kuramata A, Masui T and Yamakoshi S 2013 *Appl. Phys. Express* **6** 086502
[22] Lee M H and Peterson R L 2019 *APL Mater.* **7** 022524
[23] Tran F and Blaha P 2009 *Phys. Rev. Lett.* **102** 226401
[24] van Setten M J, Giantomassi M, Bousquet E, Verstraete M J, Hamann D R, Gonze X and Rignanese G M 2018 *Comput. Phys. Commun.* **226** 39
[25] Reeves G K and Harrison H B 1982 *IEEE Electron Dev. Lett.* **3** 111
[26] Kurtz R L and Henrich V E 1998 *Surf. Sci. Spectra* **5** 179
[27] Egerton R F 2008 *Rep. Prog. Phys.* **72** 016502
[28] Hofer F, Schmidt F, Grogger W and Kothleitner G 2015 *Proceedings of the IOP Conference Series: Materials Science and Engineering* (Portorož: IOP Publishing Ltd) pp. 3–7
[29] Henderson G S, Liu X and Fleet M E 2002 *Phys. Chem. Miner.* **29** 32
[30] Matsumoto T, Aoki M, Kinoshita A and Aono T 1974 *J. Appl. Phys.* **13** 1578
[31] Qian L X, Wu Z H, Zhang Y Y, Lai P T, Liu X Z and Li Y R 2017 *ACS Photon.* **4** 2203
[32] Dang J N, Zheng S W, Chen L and Zheng T 2019 *Chin. Phys. B* **28** 016301
[33] Greenwood N N and Earnshaw A 2012 *Elements* (Que) (Elsevier)
[34] Hou J, Guo R, Su J, Du Y, Lin Z, Zhang J, Hao Y and Chang J 2021 *Phys. Chem. Chem. Phys.* **23** 5975
[35] Stradi D, Martinez U, Blom A, Brandbyge M and Stokbro K 2016 *Phys. Rev. B* **93** 155302
[36] Smidstrup S, Stradi D, Wellendorff J, Khomyakov P A, Vej-Hansen U G, Lee M E, Ghosh T, Jonsson E, Jonsson H and Stokbro K 2017 *Phys. Rev. B* **96** 195309